

NASA TECHNICAL NOTE



NASA TN D-6373

*C.1*

NASA TN D-6373



LOAN COPY: RETURN TO  
AFWL (DOGL)  
WRIGHT-PATTERSON AFB, N. M.

# AERODYNAMIC PROPERTIES OF ROUGH SPHERICAL BALLOON WIND SENSORS

*by*

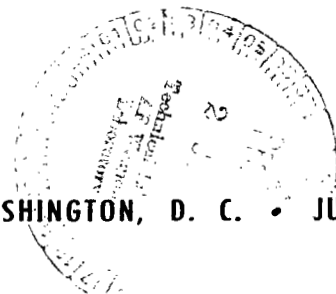
*George H. Fichtl*

*George C. Marshall Space Flight Center  
and*

*R. E. DeMandel and S. J. Krivo*

*Lockheed Missiles and Space Company*

NATIONAL AERONAUTICS AND SPACE ADMINISTRATION • WASHINGTON, D. C. • JUNE 1971





0132902

1. Report No. NASA TN D-6373	2. Government Accession No.	3. Recipient's Catalog No.	
4. Title and Subtitle Aerodynamic Properties of Rough Spherical Balloon Wind Sensors		5. Report Date June 1971	6. Performing Organization Code
7. Author(s) George H. Fichtl R. E. DeMandel and S. J. Krivo		8. Performing Organization Report No. M-169	
9. Performing Organization Name and Address George C. Marshall Space Flight Center Marshall Space Flight Center, Alabama 35812		10. Work Unit No.	
12. Sponsoring Agency Name and Address National Aeronautics and Space Administration Washington, D. C. 20546		11. Contract or Grant No.	
15. Supplementary Notes Prepared by Aero-Astroynamics Laboratory, Science and Engineering		13. Type of Report and Period Covered Technical Note	
16. Abstract		14. Sponsoring Agency Code	
<p>A first-order theory of the fluctuating lift and drag coefficients associated with the aerodynamically induced motions of rising and falling spherical balloon wind sensors is developed. The equations of motion of a sensor are perturbed about an equilibrium state in which the buoyancy force balances the mean vertical drag force. It is shown that to within first-order in perturbation quantities the aerodynamic lift force is confined to the horizontal, and the fluctuating drag force associated with fluctuations in the drag coefficient acts along the vertical. The perturbation equations are transformed with Fourier-Stieltjes integrals and the resulting equations lead to relationships between the power spectra of the aerodynamically induced velocity components and the spectra of the horizontal lift and drag coefficients.</p> <p>The aerodynamically induced motion of the Jimsphere balloon occurs predominantly in the horizontal plane, so that <math>C_{Lrms} \gg C_{Drms}</math>, where <math>C_{Lrms}</math> and <math>C_{Drms}</math> denote the root mean square horizontal lift and vertical drag coefficients. The aerodynamically induced motion is an extremely narrow-band process with essentially delta function behavior characterized by frequency <math>\omega_0</math> (rad sec<sup>-1</sup>). The nondimensional frequency <math>\omega_0 D/\bar{w}</math> (Strouhal number) and variance <math>(\sigma_u/\bar{w})^2</math> of the induced zonal or meridional components of velocity are functions of the Reynolds number based on the diameter <math>D</math> and the mean rise rate <math>\bar{w}</math> of the sensor. The experimental range of variation of the Reynolds number is <math>1.4 \times 10^5</math> to <math>6.6 \times 10^5</math>. The calculations show that <math>C_{Lrms}/\bar{C}_D \approx 0.36</math>, where <math>\bar{C}_D</math> is the mean, or zero order drag coefficient.</p> <p>The theory shows that the first-order Fourier components of the horizontally induced lift force lead the horizontally induced velocity vector, and that the induced vertical drag lags the induced vertical velocity for rising balloons and leads the falling balloons. The phase angles of the induced lift and drag associated with frequency <math>\omega_0</math> of the Jimsphere balloon are functions of the Reynolds number.</p>			
17. Key Words (Suggested by Author(s))		18. Distribution Statement  Unclassified - Unlimited	
19. Security Classif. (of this report) Unclassified	20. Security Classif. (of this page) Unclassified	21. No. of Pages 33	22. Price* \$ 3.00



# TABLE OF CONTENTS

	Page
SUMMARY .....	1
INTRODUCTION .....	2
BASIC EQUATIONS .....	3
FIRST-ORDER PERTURBATION EQUATIONS .....	4
The Lift Forces .....	4
The Drag Force .....	6
The Perturbation Equations .....	7
FOURIER-STIELTJES REPRESENTATION AND rms AERODYNAMIC COEFFICIENTS .....	8
AERODYNAMIC COEFFICIENTS FOR NARROW BAND PROCESSES .	12
JIMSPHERE LIFT COEFFICIENT .....	16
PHASE ANGLES .....	22
CONCLUSIONS .....	24
REFERENCES .....	26

# LIST OF ILLUSTRATIONS

Figure	Title	Page
1.	Power spectra of the zonal, meridional, and vertical components of velocity of the Jimsphere balloon observed at 1300 u. t. on December 23, 1964 for the height interval $4.4 < z < 5.4$ km . . . . .	13
2.	The response function used to filter the Jimsphere velocity data to isolate the aerodynamically induced balloon motion . . .	13
3.	Example of isolated aerodynamically induced Jimsphere balloon velocity components . . . . .	14
4.	The nondimensional spectrum $\omega \Phi_u(\omega)$ as a function of $\omega/\omega_0$ for $\alpha = 0.00906$ . . . . .	19
5.	The peak frequency $\omega_0/2\pi$ of the aerodynamically induced motion of the Jimsphere as a function of altitude . . . . .	19
6.	The variance $\sigma_u^2$ of the aerodynamically induced motion of the Jimsphere as a function of altitude . . . . .	20
7.	The Strouhal number $S$ of the Jimsphere balloon as a function of the Reynolds number $Re$ . . . . .	20
8.	The nondimensional zonal or meridional velocity variance $(\sigma_u/\bar{w})^2$ as a function of the Reynolds number $Re$ . . . . .	21
9.	The nondimensional time constant $\tau$ of the Jimsphere as a function of Reynolds number $Re$ . . . . .	21

## LIST OF ILLUSTRATIONS (Concluded)

Figure	Title	Page
10.	The mean drag coefficient $\bar{C}_D$ and the rms lift coefficient $C_{Lrms}$ as functions of the Reynolds number Re. . . . .	21
11.	The phase angles $\chi_1$ and $\chi_2$ of the Fourier components of the first-order aerodynamically induced horizontal lift and vertical drag forces as functions of $\omega T$ . . . . .	23
12.	The phase angles $\chi_1(S\tau)$ and $\chi_2(S\tau)$ of the Fourier components associated with the first-order aerodynamically induced horizontal lift and vertical drag forces as functions of the Reynolds number for the Jimsphere wind sensor. . . . .	24

# AERODYNAMIC PROPERTIES OF ROUGH SPHERICAL BALLOON WIND SENSORS

## SUMMARY

A first-order theory of the fluctuating lift and drag coefficients associated with the aerodynamically induced motions of rising and falling spherical balloon wind sensors is developed. The equations of motion of a sensor are perturbed about an equilibrium state in which the buoyancy force balances the mean vertical drag force. It is shown that to within first-order in perturbation quantities the aerodynamic lift force is confined to the horizontal, and the fluctuating drag force associated with fluctuations in the drag coefficient acts along the vertical. The perturbation equations are transformed with Fourier-Stieltjes integrals and the resulting equations lead to relationships between the power spectra of the aerodynamically induced velocity components and the spectra of the horizontal lift and drag coefficients.

The aerodynamically induced motion of the Jimsphere balloon occurs predominantly in the horizontal plane, so that  $C_{Lrms} \gg C_{Drms}$ , where  $C_{Lrms}$  and  $C_{Drms}$  denote the root mean square horizontal lift and vertical drag coefficients. The aerodynamically induced motion is an extremely narrow-band process with essentially delta function behavior characterized by frequency  $\omega_0$  (rad sec<sup>-1</sup>). The nondimensional frequency  $\omega_0 D / \bar{w}$  (Strouhal number) and variance  $(\sigma_u / \bar{w})^2$  of the induced zonal or meridional components of velocity are functions of the Reynolds number based on the diameter  $D$  and the mean rise rate  $\bar{w}$  of the sensor. The experimental range of variation of the Reynolds number is  $1.4 \times 10^5$  to  $6.6 \times 10^5$ . The calculations show that  $C_{Lrms} / \bar{C}_D \approx 0.36$ , where  $\bar{C}_D$  is the mean, or zero order drag coefficient.

The theory shows that the first-order Fourier components of the horizontally induced lift force lead the horizontally induced velocity vector, and that the induced vertical drag lags the induced vertical velocity for rising balloons and leads for falling balloons. The phase angles of the induced lift and drag associated with frequency  $\omega_0$  of the Jimsphere balloon are functions of the Reynolds number.

# INTRODUCTION

In the continuing pursuit of high quality wind data derived from measurements of balloon motions, three factors must be considered: (1) the response of the wind sensor to the environmental wind, (2) the accuracy of the tracking system, and (3) the aerodynamically induced motions of the sensor. This report is concerned with the third factor. Aerodynamically induced balloon motions produced by aerodynamic lift forces normal to the velocity vector of the air relative to the balloon are the result of the shedding of vorticity. Clearly, these induced motions introduce errors in the wind calculations. The physical characteristics of the balloon (shape, weight, distribution of mass, etc.) and the dynamic and thermodynamic properties of the air are the factors that control the induced sensor motion. To filter the induced motions from the balloon position measurements in an optimum manner, it is necessary that their spectral properties be known. These spectral properties can be specified in terms of the spectra of the aerodynamic lift and drag force coefficients. Once the power spectra of the aerodynamic coefficients are known, it is possible, in principle, to develop filters which can remove the aerodynamically induced motion from balloon tracking data. Knowledge of the coefficients will also aid in the design of meteorological balloons.

The purpose of this report is twofold: (1) to develop a linear perturbation theory of balloon motion, whereby it is possible to calculate spectra of the aerodynamic coefficients from self-induced balloon velocity spectra, and (2) to apply this theory to extend our present knowledge of the aerodynamic properties of roughened, spherical, balloon wind sensors like the Jimsphere.

The Jimsphere, a roughened balloon two meters in diameter, is widely used in the aerospace and meteorological communities to obtain accurate, high resolution measurements of the wind profile in the first 18 km of the atmosphere. An internal pressure of about 5 mb is maintained to insure constant volume. The 398 conical roughness elements, each approximately 7.5 cm wide at the base and 7.5 cm high, serve to control vortex shedding in the supercritical Reynolds number region below 11 km; i. e., they decrease the spectral bandwidth of aerodynamically induced motions.

## BASIC EQUATIONS

The basic equations of motion which govern the motion of a balloon or falling sphere wind sensor are given by the vector equation

$$m \frac{d\vec{V}}{dt} = \frac{1}{2} \rho C_D A |\vec{V}_e - \vec{V}| (\vec{V}_e - \vec{V}) + \frac{1}{2} \rho \vec{C}_L A |\vec{V}_e - \vec{V}|^2 + m_a \frac{d}{dt} (\vec{V}_e - \vec{V}) - (m - m_o) g \vec{k} \quad , \quad (1)$$

where  $m$ ,  $m_a$ ,  $A$ ,  $\vec{C}_L$ , and  $C_D$  denote the mass, apparent mass, cross-sectional area, the lift coefficient vector, and drag coefficient of the sensor, respectively. The symbol  $m_o$  is the mass of the air displaced by the sensor,  $g$  is the acceleration of gravity,  $\rho$  is the density of the atmosphere, and  $t$  is the time. The quantities  $\vec{V}$  and  $\vec{V}_e$  denote the velocity vectors of the sensor and the environment, and are given by

$$\vec{V} = u \vec{i} + v \vec{j} + w \vec{k} \quad (2)$$

$$\vec{V}_e = u_e \vec{i} + v_e \vec{j} + w_e \vec{k} \quad , \quad (3)$$

where  $\vec{i}$ ,  $\vec{j}$ , and  $\vec{k}$  denote unit vectors in the zonal ( $x$ ), meridional ( $y$ ), and vertical ( $z$ ) directions, and  $u$ ,  $v$ ,  $w$  and  $u_e$ ,  $v_e$ ,  $w_e$  denote the corresponding velocity components of the sensor and environment.

The first and second terms on the right-hand side of (1) represent the drag and lift forces. The drag force is parallel and opposite in direction to the wind vector relative to the balloon ( $\vec{V}_e - \vec{V}$ ). The lift force is perpendicular to the relative wind vector. The third term represents the apparent mass effect [1], and the fourth term the buoyant force. If the mass of the air displaced by the sensor is greater than the mass of the sensor ( $m < m_o$ ), the balloon will experience a positive buoyant force. Conversely, if  $m$  is greater than  $m_o$ , the sensor will experience a negative buoyant force. If  $m$  equals  $m_o$ , the buoyant force vanishes and the balloon is said to be neutral.

## FIRST-ORDER PERTURBATION EQUATIONS

The environmental wind is assumed to be composed of two parts: (1) a constant basic state horizontal flow, and (2) a superimposed velocity perturbation, so that

$$\left. \begin{aligned} u_e(t) &= \bar{u}_e + u'_e(t) \\ v_e(t) &= \bar{v}_e + v'_e(t) \\ w_e(t) &= w'_e(t) \end{aligned} \right\} \quad (4)$$

The overbars and primes denote the basic state and fluctuating parts of the wind. Similarly, the velocity components of the sensor are represented by

$$\left. \begin{aligned} u(t) &= \bar{u} + u'(t) \\ v(t) &= \bar{v} + v'(t) \\ w(t) &= \bar{w} + w'(t) \end{aligned} \right\} \quad (5)$$

Unlike the assumed environment, the sensor has a mean vertical velocity equal to  $\bar{w}$ . One assumes that the perturbation quantities in equations (4) and (5) are infinitesimal or sufficiently small so that second- and higher-order terms in perturbation quantities can be neglected with respect to first-order terms. Furthermore, it is assumed that the horizontal mean motion of the sensor is in equilibrium with the mean flow of the environment; thus,

$$\left. \begin{aligned} \bar{u} &= \bar{u}_e \\ \bar{v} &= \bar{v}_e \end{aligned} \right\} \quad (6)$$

### The Lift Forces

The aerodynamic lift forces which act in a plane perpendicular to the relative wind vector are a result of vortex shedding and instability of the wake. The magnitude and direction of these forces vary in time and are responsible for the aerodynamically induced motions exhibited by wind sensors like the

ROSE [2,3] and the Jimsphere [4] balloons. The lift coefficient vector is given by

$$\vec{C}_L = C_{Lx} \vec{i} + C_{Ly} \vec{j} + C_{Lz} \vec{k} \quad , \quad (7)$$

where  $C_{Lx}$ ,  $C_{Ly}$ , and  $C_{Lz}$  are the lift coefficients of the x, y, and z components of the lift force vector. The coefficients are functions of time and will be treated as perturbation quantities. As mentioned previously, the lift vector acts in a plane perpendicular to the relative wind vector, and the orientation of this plane is defined by the following unit vectors which are parallel to the lift force plane:

$$\vec{N}_1 = \frac{\vec{i} \times (\vec{V}_e - \vec{V})}{|\vec{i} \times (\vec{V}_e - \vec{V})|} \quad , \quad (8)$$

$$\vec{N}_2 = \frac{\vec{j} \times (\vec{V}_e - \vec{V})}{|\vec{j} \times (\vec{V}_e - \vec{V})|} \quad . \quad (9)$$

Substitution of the perturbation expansion equations (4) and (5) into equations (8) and (9) and utilization of equation (6) yields, to within first-order,

$$\vec{N}_1 = \frac{\bar{w}}{|\bar{w}|} \left\{ \vec{j} + \frac{v'_e - v'}{\bar{w}} \vec{k} \right\} \quad , \quad (10)$$

$$\vec{N}_2 = \frac{\bar{w}}{|\bar{w}|} \left\{ \vec{i} + \frac{u'_e - u'}{\bar{w}} \vec{k} \right\} \quad . \quad (11)$$

These results show that the plane of the lift force is tilted slightly from the horizontal plane. The lift coefficient vector can be written as

$$\vec{C}_L = \frac{|\bar{w}|}{\bar{w}} \left( C_1 \vec{N}_1 + C_2 \vec{N}_2 \right) \quad . \quad (12)$$

The components of this vector can be related to the components as given by equation (7) by combining equations (10), (11), and (12), to yield:

$$\vec{C}_L = C_2 \vec{i} + C_1 \vec{j} + \left[ \left( \frac{v'_e - v'}{\bar{w}} \right) C_1 + \left( \frac{u'_e - u}{\bar{w}} \right) C_2 \right] \vec{k} \quad (13)$$

Comparison of equation (13) with equation (7) shows that  $C_2 = C_{Lx}$ ,  $C_1 = C_{Ly}$ , and that  $C_{Lz}$  is therefore a second-order perturbation quantity, so that the first-order lift coefficient vector is given by

$$\vec{C}_L = C_{Lx} \vec{i} + C_{Ly} \vec{j} \quad (14)$$

This result shows the first-order lift coefficient vector to be in the horizontal plane.

Substitution of the perturbation expansion equations (4) and (5) into the lift force term in equation (1) and utilization of equations (6) and (14) yield the first-order lift force

$$\vec{F}_L = \frac{1}{2} \rho A \bar{w}^2 \left( C_{Lx} \vec{i} + C_{Ly} \vec{j} \right) \quad (15)$$

## The Drag Force

The drag coefficient can be represented in terms of a mean value  $\bar{C}_D$  and a superimposed perturbation  $C'_D$ :

$$C_D = \bar{C}_D + C'_D \quad (16)$$

Substitution of equations (4), (5), and (16) into the drag force term in equation (1) yields, to within first-order in perturbation quantities,

$$\begin{aligned} \vec{F}_D = & - \frac{1}{2} \rho A \bar{C}_D |\bar{w}| \bar{w} \vec{k} + \frac{1}{2} \rho A \bar{C}_D |\bar{w}| \left[ (u'_e - u) \vec{i} + (v'_e - v) \vec{j} \right. \\ & \left. + 2(w'_e - w) \vec{k} \right] - \frac{1}{2} \rho A C'_D |\bar{w}| \bar{w} \vec{k} \quad (17) \end{aligned}$$

The first term on the right-hand side of equation (17) is the mean drag force. The second term is the contribution to the drag force resulting from perturbations in the relative wind vector, and the third term is the contribution resulting from fluctuations in the drag coefficient.

## The Perturbation Equations

Substitution of equations (4), (5), (15), and (17) into equation (1) yields the linear perturbation equations that govern the balloon motion:

$$m \frac{du'}{dt} = \frac{1}{2} \rho A \bar{C}_D |\bar{w}| (u'_e - u') + \frac{1}{2} \rho A C_{Lx} \bar{w}^2 + m_a \frac{d}{dt} (u'_e - u') \quad (18)$$

$$m \frac{dv'}{dt} = \frac{1}{2} \rho A \bar{C}_D |\bar{w}| (v'_e - v') + \frac{1}{2} \rho A C_{Ly} \bar{w}^2 + m_a \frac{d}{dt} (v'_e - v') \quad (19)$$

$$m \frac{dw'}{dt} = \rho A \bar{C}_D |\bar{w}| (w'_e - w') - \frac{1}{2} \rho A \bar{w} |\bar{w}| C'_D + m_a \frac{d}{dt} (w'_e - w') - \frac{1}{2} \rho A \bar{C}_D |\bar{w}| \bar{w} - (m - m_o) g \quad (20)$$

In deriving equations (18), (19), and (20), it was assumed that the environmental wind field has negligible horizontal and temporal variations; i. e.,  $\bar{V}'_e$  is a function of altitude  $z$  only, so that the derivatives of the environmental wind components with respect to  $t$  in equations (18), (19), and (20) are the changes in the environmental wind as would be seen by an observer attached to the balloon (see Reference 5 for more details).

According to the theory of linear perturbation expansions, terms of like order balance, so that

$$\frac{1}{2} \rho A \bar{C}_D |\bar{w}| \bar{w} = (m_o - m) g \quad (21)$$

which permits equation (20) to be expressed as

$$m \frac{dw'}{dt} = \rho A \bar{C}_D |\bar{w}| (w'_e - w') - \frac{1}{2} \rho A \bar{w} |\bar{w}| C'_D + m_a \frac{d}{dt} (w'_e - w'). \quad (22)$$

The basic equations (18), (19), and (22) will be used in the analysis that follows. In these equations, the lift forces are confined to the horizontal plane, and the fluctuating portion of the drag force resulting from fluctuations in the drag coefficient is confined to the vertical direction.

## FOURIER-STIELTJES REPRESENTATION AND rms AERODYNAMIC COEFFICIENTS

The time-dependent quantities in equations (18), (19), and (22) can be represented with Fourier-Stieltjes integrals; i. e. ,

$$\xi(t) = \int_{-\infty}^{\infty} e^{i\omega t} dZ_{\xi}(\omega) \quad , \quad (23)$$

where  $\xi(t)$  is a time-dependent quantity, and  $dZ_{\xi}(\omega)$  is the complex Fourier amplitude of  $\xi(t)$  at frequency  $\omega$  and is given by

$$dZ_{\xi}(\omega) = \lim_{\tau_0 \rightarrow \infty} \frac{1}{2\pi} \int_{-\tau_0}^{\tau_0} \xi(t) e^{-i\omega t} \left( \frac{1 - e^{-itd\omega}}{it} \right) dt \quad . \quad (24)$$

The equations that govern the Fourier amplitudes of the time-dependent quantities in (18), (19), and (22) are obtained by substituting their Fourier-Stieltjes representations and noting that the functions  $\exp(i\omega t)$  constitute a complete orthogonal function set, so that

$$dZ_u(\omega) = \frac{1 + i\mu\omega T}{1 + i\omega T} dZ_{u_e}(\omega) + \frac{|\bar{w}|}{\bar{C}_D} \frac{dZ_x(\omega)}{1 + i\omega T} \quad , \quad (25)$$

$$dZ_v(\omega) = \frac{1 + i\mu\omega T}{1 + i\omega T} dZ_{v_e}(\omega) + \frac{|\bar{w}|}{\bar{C}_D} \frac{dZ_y(\omega)}{1 + i\omega T} \quad , \quad (26)$$

$$dZ_w(\omega) = \frac{2 + i\mu\omega T}{2 + i\omega T} dZ_{w_e}(\omega) - \frac{\bar{w}}{\bar{C}_D} \frac{dZ_z(\omega)}{2 + i\omega T} \quad , \quad (27)$$

where  $dZ_{u,v,w}$  and  $dZ_{u_e, v_e, w_e}$  are the Fourier amplitudes of  $u'$ ,  $v'$ ,  $w'$  and  $u'_e$ ,  $v'_e$ ,  $w'_e$ ;  $dZ_{x,y,z}$  are the Fourier amplitudes of  $C_{Lx,y}$  and  $C'_D$ . The quantities  $T$  and  $\mu$  are given by

$$T = \frac{m + m_a}{|m_o - m|} \frac{|\bar{w}|}{g}, \quad (28)$$

$$\mu = \frac{m_a}{m + m_a}. \quad (29)$$

The power spectra of the velocity components of the balloon motion can be obtained by multiplying each of the equations (25), (26), and (27) by its complex conjugate and performing an ensemble average over all realizations; thus

$$\begin{aligned} \phi_u(\omega) = & \frac{1 + (\mu\omega T)^2}{1 + (\omega T)^2} \phi_{u_e}(\omega) + \frac{\bar{w}^2}{\bar{C}_D^2} \cdot \frac{\phi_x(\omega)}{1 + (\omega T)^2} \\ & + 2 \frac{|\bar{w}|}{\bar{C}_D} \frac{\left\{ \text{Re} \left[ \phi_{u_e^x}(\omega) \right] - \mu\omega T \text{Im} \left[ \phi_{u_e^x}(\omega) \right] \right\}}{1 + (\omega T)^2}, \end{aligned} \quad (30)$$

$$\begin{aligned} \phi_v(\omega) = & \frac{1 + (\mu\omega T)^2}{1 + (\omega T)^2} \phi_{v_e}(\omega) + \frac{\bar{w}^2}{\bar{C}_D^2} \cdot \frac{\phi_y(\omega)}{1 + (\omega T)^2} \\ & + 2 \frac{|\bar{w}|}{\bar{C}_D} \frac{\left\{ \text{Re} \left[ \phi_{v_e^y}(\omega) \right] - \mu\omega T \text{Im} \left[ \phi_{v_e^y}(\omega) \right] \right\}}{1 + (\omega T)^2}, \end{aligned} \quad (31)$$

$$\phi_w(\omega) = \frac{4 + (\mu\omega T)^2}{4 + (\omega T)^2} \phi_{w_e}(\omega) + \frac{\bar{w}^2}{\bar{C}_D^2} \cdot \frac{\phi_z(\omega)}{4 + (\omega T)^2} - 2 \frac{\bar{w}}{\bar{C}_D} \frac{\left\{ 2 \operatorname{Re}[\phi_{w_e z}(\omega)] - \mu\omega T \operatorname{Im}[\phi_{w_e z}(\omega)] \right\}}{4 + (\omega T)^2}, \quad (32)$$

where the  $\phi$ 's with a single subscript are autospectra and the  $\phi$ 's with the double subscripts are cross-spectra. Thus, for example,

$$\phi_{u_e}(\omega) d\omega = \left\langle dZ_{u_e}(\omega) dZ_{u_e}^*(\omega) \right\rangle, \quad (33)$$

$$\phi_{u_e x}(\omega) d\omega = \left\langle dZ_{u_e}(\omega) dZ_x^*(\omega) \right\rangle, \quad (34)$$

where \* denotes complex conjugation, and  $\langle \rangle$  denotes the ensemble average operator. The notations  $\operatorname{Re}(\phi)$  and  $\operatorname{Im}(\phi)$  represent the real and imaginary parts of  $\phi$ .

The first terms on the right-hand sides of equations (30), (31), and (32) are the contributions to the balloon motion spectra by the environmental wind fluctuations. These terms have been discussed in detail in Reference 5. The last terms are the contributions resulting from correlations between the aerodynamic coefficients and the environmental wind fluctuations. It is assumed that these cross-spectral terms will vanish. The second terms are the contributions to the balloon motion spectra resulting from fluctuations in the aerodynamic coefficients. These terms correspond to the aerodynamically induced balloon motions. Representing these terms by  $\psi_{u,v,w}(\omega)$ , one can write

$$\phi_x(\omega) = \frac{\bar{C}_D^2}{\bar{w}^2} \left[ 1 + (\omega T)^2 \right] \psi_u(\omega), \quad (35)$$

$$\phi_y(\omega) = \frac{\bar{C}_D^2}{\bar{w}^2} \left[ 1 + (\omega T)^2 \right] \psi_v(\omega), \quad (36)$$

$$\phi_z(\omega) = \frac{\bar{C}_D^2}{\bar{w}^2} \left[ 4 + (\omega T)^2 \right] \psi_w(\omega). \quad (37)$$

The lift force is statistically isotropic in the horizontal plane; therefore,

$$\begin{aligned}\psi_{\mathbf{u}}(\omega) &= \psi_{\mathbf{v}}(\omega) \quad , \\ \phi_{\mathbf{x}}(\omega) &= \phi_{\mathbf{y}}(\omega) \quad .\end{aligned}\tag{38}$$

Thus, only one component of the lift force vector in the horizontal plane need be considered. The root mean square (rms) lift and drag coefficients can be obtained by integrating equations (35) and (37) over the domain  $-\infty < \omega < \infty$  with the result

$$C_{Lrms}^2 = \bar{C}_D^2 \frac{\sigma_u^2}{\bar{w}^2} \int_0^\infty [1 + (\omega T)^2] \Phi_u(\omega) d\omega \quad , \tag{39}$$

$$C_{Drms}^2 = \bar{C}_D^2 \frac{\sigma_w^2}{\bar{w}^2} \int_0^\infty [4 + (\omega T)^2] \Phi_w(\omega) d\omega \quad , \tag{40}$$

where  $\sigma_u$  and  $\sigma_w$  are the standard deviations of the zonal and vertical self-induced velocity components. The standard deviation of the meridional component is equal to  $\sigma_u$ . The quantities  $\Phi_u(\omega)$  and  $\Phi_w(\omega)$  are the corresponding normalized spectra referenced to the half-interval  $0 < \omega < \infty$ ,

$$\left. \begin{aligned}\Phi_u(\omega) &= 2 \frac{\psi_u(\omega)}{\sigma_u^2} \\ \Phi_w(\omega) &= 2 \frac{\psi_w(\omega)}{\sigma_w^2}\end{aligned}\right\} . \tag{41}$$

Equations (39) and (40) can be written in terms of integrals over the half-interval  $0 < \omega < \infty$  because the spectra of the aerodynamic coefficients are even functions of  $\omega$ . These equations facilitate the calculation of the rms aerodynamic coefficients from relatively simple measurements of the aerodynamically induced sensor motion.

## AERODYNAMIC COEFFICIENTS FOR NARROW BAND PROCESSES

The self-induced balloon motions of rough spherical sensors like the Jimsphere are high frequency, narrow band processes. Figure 1 contains spectra of the zonal, meridional, and vertical components of velocity of a Jimsphere wind sensor for the altitude interval  $4.4 < z < 5.4$  km calculated from FPS-16 radar data taken between 1400 to 1500 u. t. on December 23, 1964. The zonal and meridional spectra have peaks at approximately 0.21 Hz. These peaks are attributed to the self-induced balloon motion which results from the fluctuating, aerodynamic lift force. The absence of a pronounced spectral peak in the vertical velocity spectrum at, or close to, 0.21 Hz precludes the existence of a significant vertical component of self-induced balloon motion and implies that  $C_{Drms} \ll C_{Lrms}$ . This means the self-induced balloon motion is confined primarily to the horizontal. If the spectral peaks in Figure 1 are associated with a self-induced spiral motion as observed by Scoggins [4], then the zonal and meridional components should be out of phase by 90 degrees. To verify that this is indeed the case, the Jimsphere velocity data were filtered with a Martin-Graham [6] band pass filter, the response function of which is shown in Figure 2. The example of the filtered data given in Figure 3 clearly shows that the zonal and meridional balloon velocities are out of phase by 90 degrees. The filtered vertical velocity data, also in Figure 3, show that the vertical self-induced motion, if it exists, is very small.

A particularly useful way to represent a narrow band process is with the function

$$\Phi_u(\omega) = \frac{1}{1 - F(-\omega_o/\epsilon)} \cdot \frac{e^{-\frac{(\omega - \omega_o)^2}{2\epsilon^2}}}{\epsilon (2\pi)^{1/2}}, \quad 0 < \omega < \infty, \quad (42)$$

where

$$F(-\omega_o/\epsilon) = 1 - \int_{-\omega_o/\epsilon}^{\infty} \frac{1}{(2\pi)^{1/2}} e^{-\xi^{1/2}} d\xi. \quad (43)$$

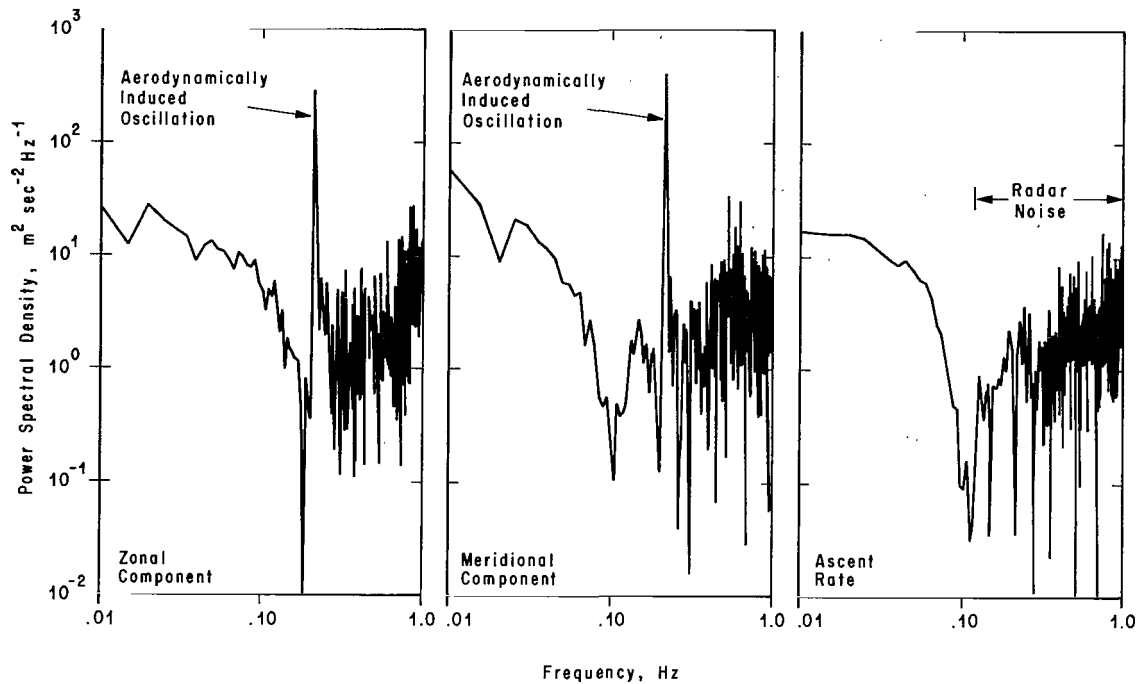


Figure 1. Power spectra of the zonal, meridional, and vertical components of velocity of the Jimsphere balloon observed at 1300 u. t. on December 23, 1964 for the height interval  $4.4 < z < 5.4$  km.

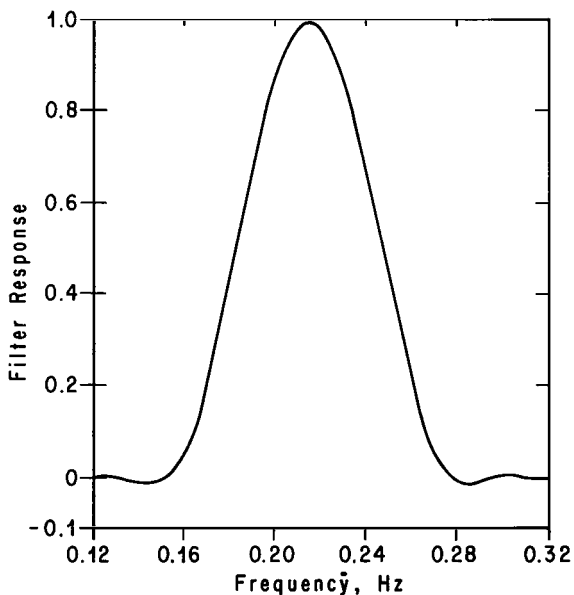


Figure 2. The response function used to filter the Jimsphere velocity data to isolate the aerodynamically induced balloon motion.

The maximum value of  $\Phi_u(\omega)$  occurs at  $\omega = \omega_0$ , and  $\epsilon$  is a measure of the width of the spectrum. If  $\epsilon \rightarrow 0$ , then

$$\Phi_u(\omega) \rightarrow \delta(\omega - \omega_0) \quad , \quad (44)$$

where  $\delta(\omega - \omega_0)$  is the Dirac delta function [7].

Substitution of equation (42) into equation (39) yields

$$C_{Lrms} = C_D^2 \frac{\sigma_u^2}{w^2} \left\{ \left[ 1 + T^2 (\omega_0^2 + \epsilon^2) \right] + \frac{T^2 \left[ 2\epsilon \omega_0 f(-\omega_0/\epsilon) - \epsilon^2 f'(-\omega_0/\epsilon) \right]}{1 - F(-\omega_0/\epsilon)} \right\} \quad (45)$$

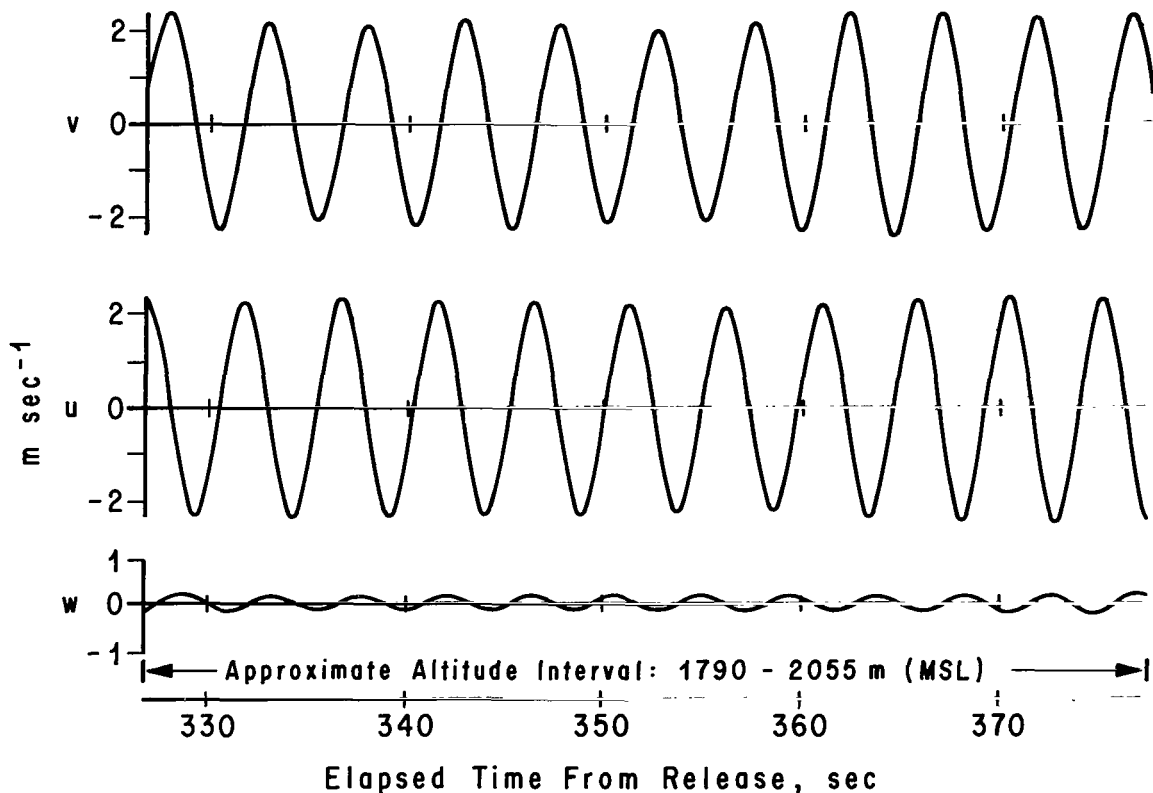


Figure 3. Example of isolated aerodynamically induced Jimsphere balloon velocity components. (The zonal and meridional velocity components are out of phase by 90 degrees. The vertical component of the induced velocity vector is extremely small.)

where

$$f(\zeta) = \frac{1}{(2\pi)^{1/2}} e^{-\zeta^{1/2}} \quad (46)$$

and  $f'(-\omega_0/\epsilon)$  denotes the derivative of  $f(\zeta)$  with respect to  $\zeta$  and evaluation at  $\zeta = -\omega_0/\epsilon$ . If the widths of the balloon motion spectra are sufficiently narrow, such that  $\omega_0/\epsilon \geq 3$  say, the quantities  $f(-\omega_0/\epsilon)$  and  $f'(-\omega_0/\epsilon)$  approach zero, so that the second term on the right-hand side of equation (45) can be neglected in comparison to the first term. Thus, the approximate expression for the rms lift coefficient is

$$C_{Lrms}^2 = \bar{C}_D^2 \frac{\sigma_u^2}{w^2} \left[ 1 + T^2 (\omega_o^2 + \epsilon^2) \right] \quad (47)$$

Furthermore, if the balloon motion spectrum is sufficiently narrow, such that  $\epsilon \ll \omega_o$ , then

$$C_{Lrms}^2 = \bar{C}_D^2 \frac{\sigma_u^2}{w^2} \left[ 1 + (\omega_o T)^2 \right] \quad (48)$$

This corresponds to the case in which  $\Phi_u(\omega)$  is a Dirac delta function as given by equation (44).

Even though the magnitude of the vertical self-induced balloon motion is extremely small, an estimate of an upper bound on  $C_{Drms}$  can be obtained with the data in Figure 3. The result that corresponds to equation (47) for the rms drag coefficient is

$$C_{Drms}^2 = \bar{C}_D^2 \frac{\sigma_w^2}{w^2} \left[ 4 + T^2 (\omega_o^2 + \epsilon^2) \right] \quad (49)$$

The ratio between the rms drag and lift coefficients is

$$\frac{C_{Drms}}{C_{Lrms}} = \frac{\sigma_w}{\sigma_u} \left[ \frac{4 + T^2 (\omega_o^2 + \epsilon^2)}{1 + T^2 (\omega_o^2 + \epsilon^2)} \right]^{1/2} \quad (50)$$

The ratio  $\sigma_w/\sigma_u$  is approximately equal to 0.1, at most, according to the data in Figure 3. In addition, an upper bound value of the coefficient of  $\sigma_w/\sigma_u$  in equation (50) is 2; therefore,  $C_{Drms} \leq 0.2 C_{Lrms}$ . In all probability, the radar error contained in the w' time history in Figure 3 accounts for at least 50 percent of the signal; thus, a more reasonable estimate is  $C_{Drms} \leq 0.1 C_{Lrms}$ , which seems to verify the earlier conjecture that  $C_{Drms} \ll C_{Lrms}$ . The radar error is small in comparison to the signals associated with horizontal components of the aerodynamically induced motion.

## JIMSPHERE LIFT COEFFICIENT

To determine the rms lift coefficient of the Jimsphere wind sensor, three dual radar tracks of the Jimsphere, tracked with the FPS-16 radar, were selected for analysis. The measurements were made between 1300 to 1500 u. t. on December 23, 1964, December 18, 1967, and March 19, 1968, at the Kennedy Space Center, Florida. These tests will be referred to as flights 1, 2, and 3, respectively. The measurements extended over the altitude interval 0.5 to 16 km. The radar provided range and elevation and azimuth angle data on the location of the balloon at 0.1-sec intervals. These data were converted to Cartesian coordinates and corrected for the curvature of the earth. The Cartesian coordinates were differenced over 0.2-sec intervals to yield estimates of the zonal, meridional, and vertical velocities of the balloon at 0.1-sec intervals. The resulting velocity time histories were used to calculate the rms lift coefficient of the Jimsphere balloon.

As a constant diameter spherical wind sensor ascends through the atmosphere, the Reynolds number

$$\text{Re} = \frac{|\bar{w}|D}{\nu} \quad (51)$$

decreases because the coefficient of kinematic viscosity  $\nu$  usually increases with height while the rise rate  $|\bar{w}|$  usually has a slow decrease with height. The quantity  $D$  is the diameter of the sensor. Since the aerodynamic properties of spheres depend on the Reynolds number, one should expect a dependence of the lift coefficient on altitude. Accordingly, the balloon velocity time histories were divided into 1-km segments to calculate the rms lift coefficients of the Jimsphere.

Power spectra of the zonal, meridional, and vertical components of velocity were calculated for each time history segment. This resulted in 15 spectra for each component of velocity for each balloon track, or a total of 270 spectra. The vertical velocity spectra looked like the example shown in Figure 1, and thus did not reveal any obvious vertical aerodynamically induced motion. It was assumed that the zonal and meridional self-induced velocity spectra are of the form given by equation (42). This representation proved to be reasonable. Rogers and Camnitz [8] analyzed line-of-sight velocity spectra of the 2-meter ROSE balloon calculated with Doppler radar measurements and found that equation (42) is a valid representation of the aerodynamically induced balloon motion. In the case of the Jimsphere balloon,  $F(-\omega_0/\epsilon)$  is approximately 0; thus, one may write

$$\Phi_u(\omega) = \frac{1}{(2\pi)^{1/2} \epsilon} e^{-(\omega - \omega_o)^2 / 2 \epsilon^2} \quad (52)$$

To develop a model of the aerodynamically induced velocity spectra, it was assumed that  $\omega_o \Phi_u(\omega)$  is a universal function of  $\omega/\omega_o$ . The nondimensional frequency or Strouhal number<sup>1</sup> of the sensor

$$S = \frac{\omega_o D}{|\bar{w}|} \quad (53)$$

and the nondimensional variance  $(\sigma_u/\bar{w})^2$  are universal functions of the Reynolds number:

$$\left. \begin{aligned} S &= F_1(\text{Re}) \\ \left(\frac{\sigma_u}{\bar{w}}\right)^2 &= F_2(\text{Re}) \end{aligned} \right\} \quad (54)$$

The nondimensional power spectrum is given by

$$\omega_o \Phi_u(\omega) = \frac{1}{(2\pi)^{1/2} \alpha} e^{-(1 - \omega/\omega_o)^2 / 2\alpha^2} \quad (55)$$

where

$$\alpha = \frac{\epsilon}{\omega_o} \quad (56)$$

The quantity  $\alpha$  is a universal constant. The numerical value of  $\alpha$  was obtained by determining that value of  $\omega/\omega_o$ ,  $\omega^*/\omega_o$ , say, at which  $\omega_o \Phi_u(\omega)$  is equal to one-tenth of the peak value; that is,  $(\omega^*) = 0.1 \omega_o \Phi_u(\omega_o) = 0.1 [(2\pi)^{1/2} \alpha]^{-1}$ . Substitution of  $\omega^*/\omega_o$  into equation (55) yields the result

1. Usually the Strouhal number refers to the nondimensional frequency of the dominant Fourier component in the wake. Here, however, it is used to denote the nondimensional frequency of the sensor.

$$\alpha = \frac{1 - \omega^*/\omega_o}{(2 \ln 10)^{1/2}} \quad (57)$$

The quantity  $\alpha$  was calculated for each horizontal spectrum with equation (57). The various values of  $\alpha$  showed no dependence on height and thus Reynolds number. The expected value of  $\alpha = 0.00906$ . Figure 4 is a plot of the nondimensional spectrum  $\omega_o \Phi_u(\omega)$  as a function of  $\omega/\omega_o$  for  $\alpha = 0.00906$ .

The peak frequency  $\omega_o$  and the area  $\sigma_u^2$  under the aerodynamically induced spectral peak were used to calculate the nondimensional functions  $F_1(\text{Re})$  and  $F_2(\text{Re})$ . Figures 5 and 6 are plots of  $\omega_o/2\pi$  and  $\sigma_u^2$  as functions of altitude. The plotted data are the expected values of  $\omega_o/2\pi$  and  $\sigma_u^2$  for each 1-km segment of each balloon flight obtained by averaging the corresponding zonal and meridional values. A smooth line was drawn through each set of data. The smoothed values of  $\omega_o/2\pi$  and  $\sigma_u^2$ , the standard profile of  $\bar{w}$  as a function of altitude calculated by DeMandel and Krivo [9], and the standard atmosphere profile of  $\nu$  [10] were used to calculate the nondimensional functions  $F_1(\text{Re})$  and  $F_2(\text{Re})$ . These functions correspond to the Strouhal number and the nondimensional zonal or meridional velocity variance  $(\sigma_u/\bar{w})^2$  (Figs. 7 and 8). Figure 7 shows that the Strouhal number has a typical value equal to 0.55 with a maximum value approximately equal to 0.60 at  $\text{Re} = 2.5 \times 10^5$ . Figure 8 shows that the nondimensional variance is a monotonically increasing function of the Reynolds number in the interval  $1.4 \times 10^5 < \text{Re} < 6.7 \times 10^5$  with values ranging between 0.03 and 0.092.

The final parameters needed to calculate the rms lift coefficient are the nondimensional time constant

$$\tau = \frac{T|\bar{w}|}{D} \quad (58)$$

and the mean drag coefficient  $\bar{C}_D$  of the Jimsphere. Fichtl [5] calculated  $T$  as a function of altitude for the Jimsphere. Substitution of  $T$  into equation (58) with the mean rise rate profile of DeMandel and Krivo [9] and plotting the resulting values of  $\tau$  as a function of Reynolds number yields the curve in Figure 9. Figure 10 contains a plot of  $\bar{C}_D$  as a function of Reynolds number.

In view of the extremely small values of  $\alpha$  with respect to unity, one may treat the power spectra of the zonal and meridional velocity spectra of the

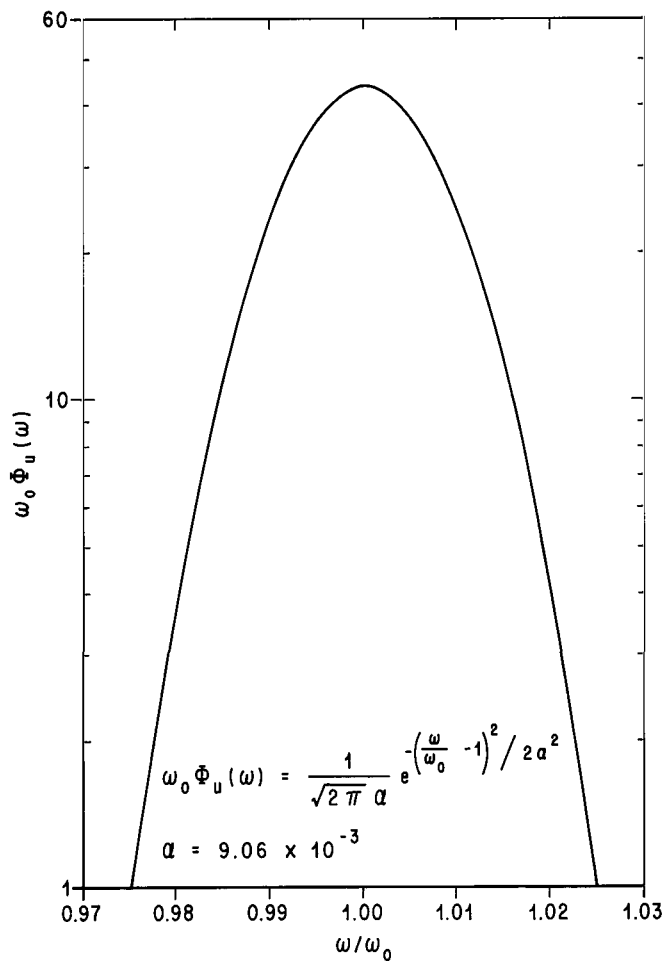


Figure 4. The nondimensional spectrum  $\omega_0 \Phi_u(\omega)$  as a function of  $\omega/\omega_0$  for  $\alpha = 0.00906$ .

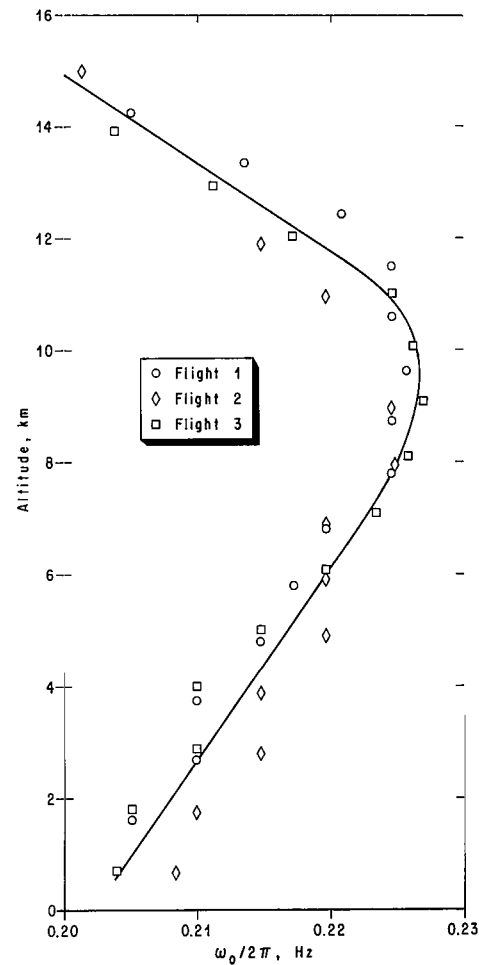


Figure 5. The peak frequency  $\omega_0/2\pi$  of the aerodynamically induced motion of the Jimsphere as a function of altitude.

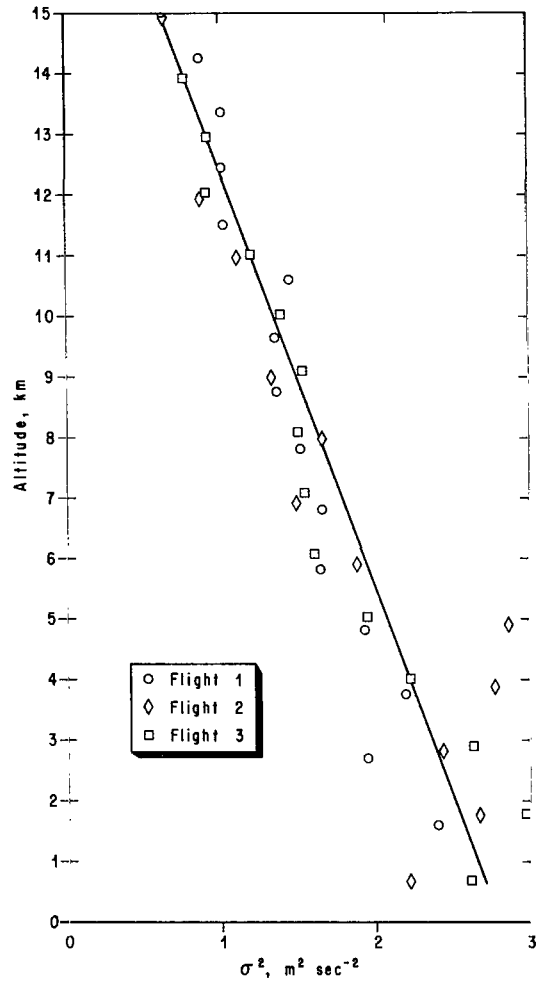


Figure 6. The variance  $\sigma_u^2$  of the aerodynamically induced motion of the Jimsphere as a function of altitude.

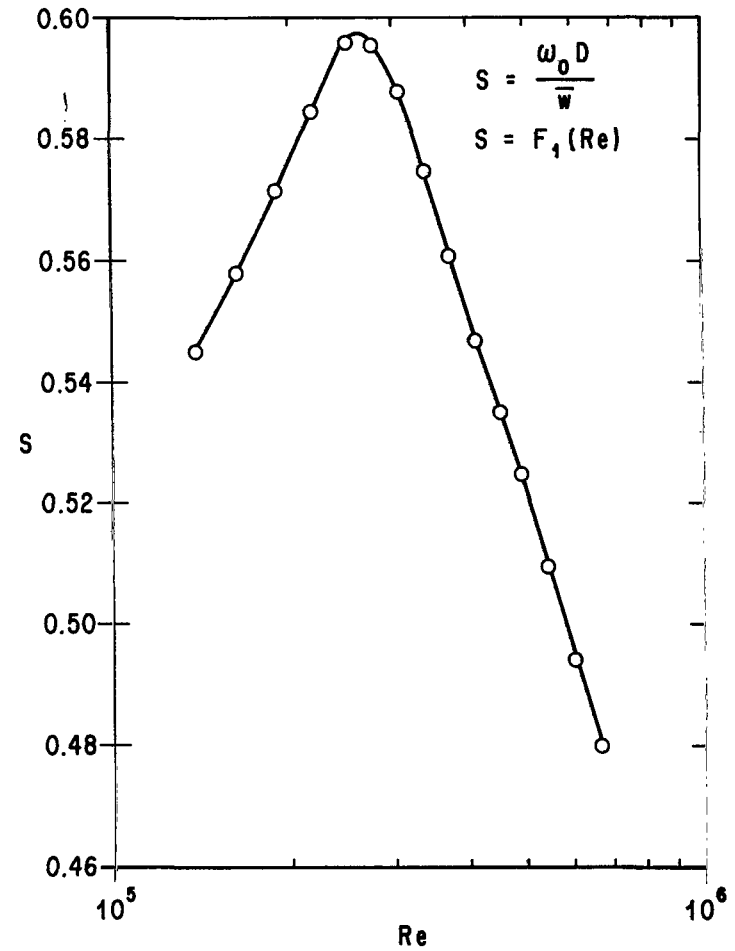


Figure 7. The Strouhal number  $S$  of the Jimsphere balloon as a function of the Reynolds number  $Re$ .

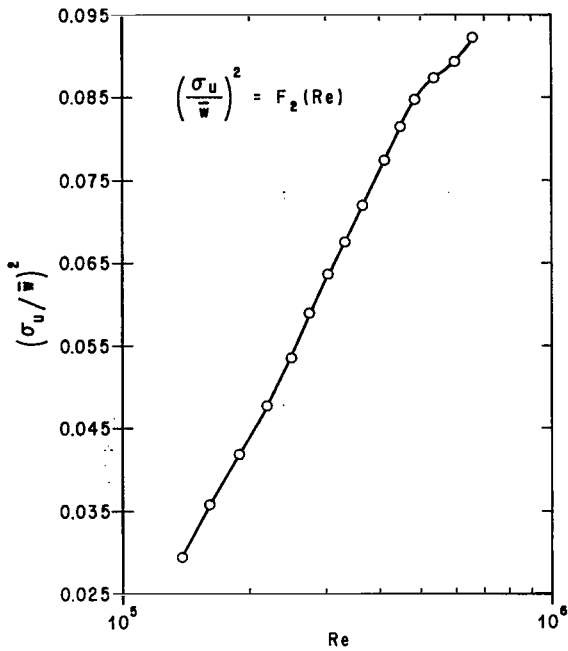


Figure 8. The nondimensional zonal or meridional velocity variance  $(\sigma_u/\bar{w})^2$  as a function of the Reynolds number  $Re$ .

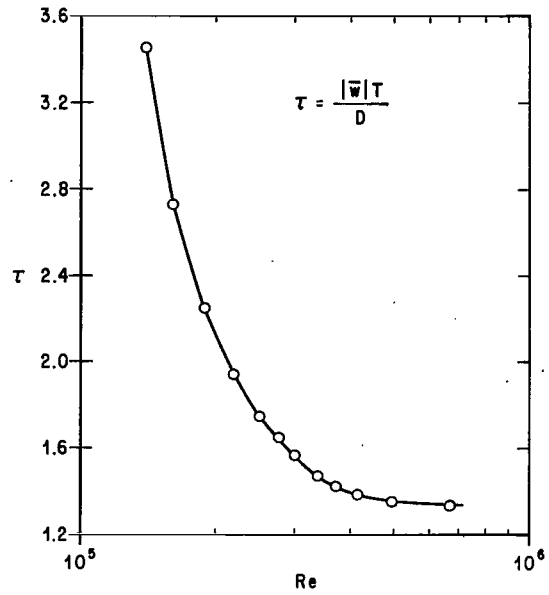


Figure 9. The nondimensional time constant  $\tau$  of the Jimsphere as a function of Reynolds number  $Re$ .

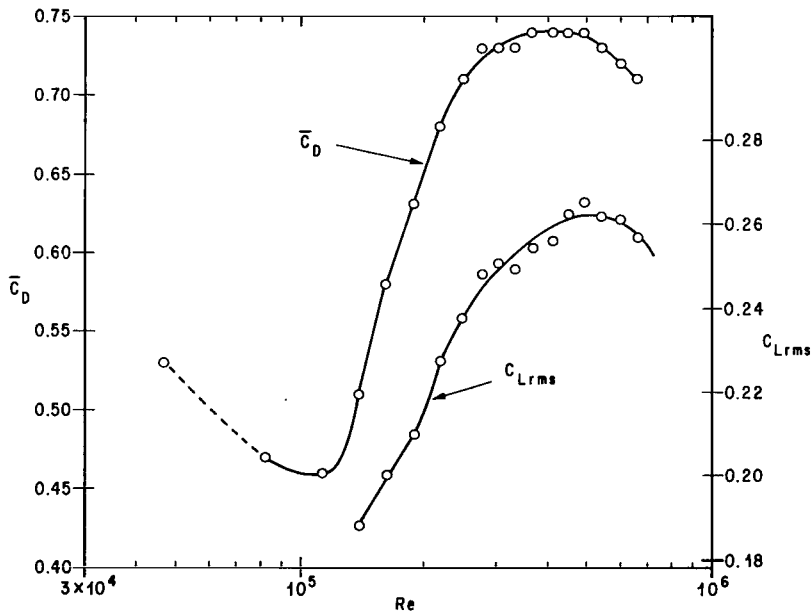


Figure 10. The mean drag coefficient  $\bar{C}_D$  and the rms lift coefficient  $C_{Lrms}$  as functions of the Reynolds number  $Re$ .

Jimsphere aerodynamically induced motion as Dirac delta functions. This means that equation (48) is applicable to the problem and can be written in terms of  $S$  and  $\tau$  as

$$C_{Lrms}^2 = \bar{C}_D^2 \frac{\sigma_u^2}{\bar{w}^2} \left[ 1 + (S\tau)^2 \right] \quad (59)$$

Substitution of  $S$ ,  $(\sigma_u/\bar{w})^2$ ,  $\tau$ , and  $\bar{C}_D$ , as given in Figures 7, 8, 9, and 10, into equation (59) yields the rms lift coefficient as a function of Reynolds number (Fig. 10). The results in Figure 10 show that the  $C_{Lrms}$  and  $\bar{C}_D$  curves tend to have somewhat similar shapes and a typical value of the ratio  $C_{Lrms}/\bar{C}_D = 0.36$ .

## PHASE ANGLES

To determine the phase angles of the fluctuating lift and drag forces relative to the aerodynamically induced balloon motion, one writes the second terms on the right-hand side of equations (25), (26), and (27) as

$$\left. \begin{aligned} dZ_{u_1} &= \frac{|\bar{w}|}{\bar{C}_D} e^{i\chi_1} \frac{dZ_x(\omega)}{[1 + (\omega T)^2]^{1/2}} \\ dZ_{v_1} &= \frac{|\bar{w}|}{\bar{C}_D} e^{i\chi_1} \frac{dZ_y(\omega)}{[1 + (\omega T)^2]^{1/2}} \\ dZ_{w_1} &= \frac{|\bar{w}|}{\bar{C}_D} e^{i\chi_2} \frac{dZ_z(\omega)}{[4 + (\omega T)^2]^{1/2}} \end{aligned} \right\} \quad (60)$$

where

$$\left. \begin{aligned} \chi_1 &= \tan^{-1}(-\omega T) \\ \chi_2 &= \frac{\pi}{2} \left( 1 + \frac{\bar{w}}{|\bar{w}|} \right) + \tan^{-1} \left( -\frac{\omega T}{2} \right) \end{aligned} \right\} \quad (61)$$

The quantities  $dZ_{u_1, v_1, w_1}$  are the Fourier amplitudes of aerodynamically induced components of velocity of the balloon. The quantity  $\chi_1$  is the phase angle of the zonal and meridional components of the induced lift force relative to the corresponding components of the induced velocity and  $\chi_2$  is the phase angle of the vertical component of the induced fluctuating drag force relative to the induced vertical velocity. These results imply that the induced aerodynamic lift force leads the corresponding induced horizontal component of velocity. For a rising balloon ( $\bar{w} > 0$ ), the induced vertical drag force lags the induced vertical velocity and vice versa for the falling balloon ( $\bar{w} < 0$ ). Figure 11 contains plots of  $\chi_1$  and  $\chi_2$  as functions of  $\omega T$  for the rising balloon case. The phase angles for the falling balloon can be obtained from Fig. 11 by subtracting  $\pi$  radians from  $\chi_2$ .

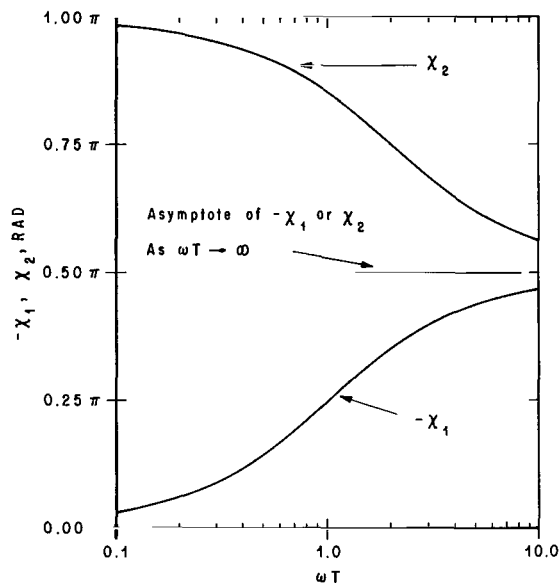


Figure 11. The phase angles  $\chi_1$  and  $\chi_2$  of the Fourier components of the first-order aerodynamically induced horizontal lift and vertical drag forces as functions of  $\omega T$  for the rising balloon ( $\bar{w} > 0$ ). For the falling balloon ( $\bar{w} < 0$ ),  $\pi$  radians must be subtracted from  $\chi_2$ .

The Jimsphere induced motion is characterized by essentially one Fourier component located at  $\omega = \omega_0$ . Thus, one writes equation (61) as

$$\left. \begin{aligned} \chi_1 &= \tan^{-1}(-S\tau) \\ \chi_2 &= \pi + \tan^{-1}\left(-\frac{S\tau}{2}\right) \end{aligned} \right\} \quad (62)$$

The quantities  $S$  and  $\tau$  are functions of the Reynolds number, so that  $\chi_1$  and  $\chi_2$  are also functions of the Reynolds number. Figure 12 gives  $\chi_1$  and  $\chi_2$  as functions of the Reynolds number for the Jimsphere wind sensor based on the data in Figures 7 and 9.

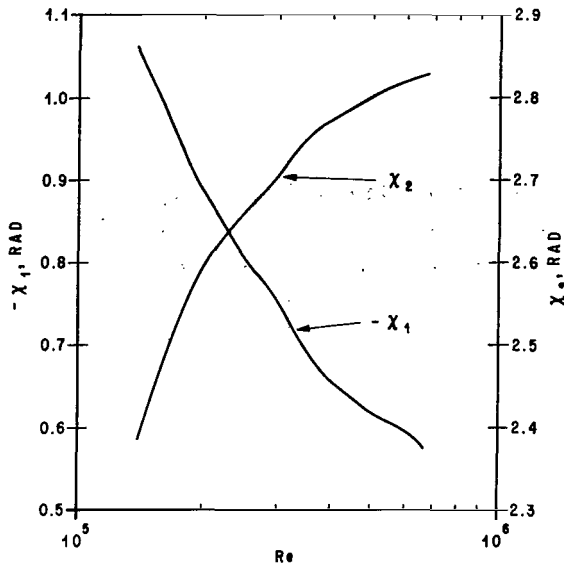


Figure 12. The phase angles  $\chi_1(S\tau)$  and  $\chi_2(S\tau)$  of the Fourier components associated with the first-order aerodynamically induced horizontal lift and vertical drag forces as functions of the Reynolds number for the Jimsphere wind sensor.

Analyses of the FPS-16 radar tracking data of the Jimsphere balloon showed that the aerodynamically induced motions are extremely narrow band processes characterized by velocity power spectra that have delta function behavior, for all practical purposes. Since aerodynamically induced motion occurs predominantly in the horizontal plane, it is concluded that the first-order rms drag coefficient is at most one-tenth of the horizontal rms lift coefficient. These results are supported by the earlier results of Scoggins [4]. It was found that the nondimensional induced zonal or meridional velocity variance, Strouhal number, and the horizontal rms lift coefficient are functions of the Reynolds number. They should also be functions of the mass ratio  $m/m_0$ , where  $m$  is the mass of the sensor and  $m_0$  is the mass of air displaced by the sensor. To determine how the Strouhal number and nondimensional velocity variance depend on  $m/m_0$  would be rather difficult because many sensor configurations would be required to cover a sufficiently wide

## CONCLUSIONS

The aerodynamic properties of rough spherical wind sensors have been established by using linear perturbation expansions of the equations of motion of a sensor and FPS-16 radar tracking data of the Jimsphere balloon. Integral relationships between the first-order rms drag and horizontal lift coefficients were obtained from the first-order perturbation equations. These relationships show that the rms lift and drag coefficients can be obtained from measurements of the mean drag coefficient, the mean vertical velocity, and the time constant of the sensor and estimates of the component velocity spectra of the aerodynamically induced balloon motion. These relationships are reduced to rather simple equations in the case of sufficiently narrow band processes. The mathematical analysis can be applied to both rough and smooth sensors.

range of values of  $m/m_0$ . The horizontal rms lift coefficient is approximately equal to  $0.36 \bar{C}_D$ .

The precise nature of the mechanism which produces the aerodynamically induced motion of rough sensors, or smooth sensors, is rather complicated. It is obvious that the wake is unstable and that vorticity is being shed from the balloon resulting in periodic x- and y-directed aerodynamic lift forces. However, the nature of the instability which results in the oscillating wake is not clear.

George C. Marshall Space Flight Center  
National Aeronautics and Space Administration  
Marshall Space Flight Center, Alabama 35812  
December 28, 1970 126-61-10-00

## REFERENCES

1. Reed, Wilmer H. , III: Dynamic Response of Rising and Falling Balloon Wind Sensors with Application to Estimates of Wind Loads on Launch Vehicles. NASA TN D-1821, The National Aeronautics and Space Administration, 1963, 31 pp.
2. Engler, N. A. : Development of Methods to Determine Wind, Density, Pressure, and Temperature From the Robin Falling Balloon. Final Report, AF 19(604)-7450, University of Dayton, 1965, 141 pp.
3. Brockman, W. E. : Small Scale Wind Shears From ROSE Balloon Tracked by AN/FPS-16 Radar. Final Report, AF 19(604)-7450, University of Dayton, 1964, 85 pp.
4. Scoggins, J. R. : Sphere Behavior and the Measurement of Wind Profiles. NASA TN D-3994, The National Aeronautics and Space Administration, 1967, 53 pp.
5. Fichtl, G. H. : The Responses of Balloon and Falling Sphere Wind Sensors in Turbulent Flows. NASA TN D-7049, The National Aeronautics and Space Administration, 1971, 26 pp.
6. DeMandel, R. , and Krivo, S. J. : Selecting Digital Filters for Application to Detailed Wind Profiles. NASA CR-61325, The National Aeronautics and Space Administration, 1969, 136 pp.
7. Lighthill, M. J. : Introduction to Fourier Analysis and Generalized Functions. Cambridge University Press, New York, New York, 1958, 79 pp.
8. Rogers, R. R. , and Camnitz, H. G. : Project Baldy, an Investigation of Aerodynamically-Induced Balloon Motions. Final Report, NAS8-11140, Cornell Aeronautical Laboratory, Inc. , 1965, 80 pp.
9. DeMandel, R. E. , and Krivo, S. J. : Radar/Balloon Measurement of Vertical Air Motions Between the Surface and 15 km, J. Appl. Meteor. , vol. 10, April 1971, pp. 313-319.
10. U. S. Standard Atmosphere Supplements. The National Aeronautics and Space Administration. U. S. Weather Bureau, The U. S. Printing Office, Washington, D. C. , 1966, 289 pp.